Extremum Seeking-Based Optimization of High Voltage Converter Modulator Rise-Time

Alexander Scheinker, *Student Member, IEEE*, Michael Bland, Miroslav Krstić, *Fellow, IEEE*, and Jeff Audia

***Abstract*— We digitally implement an extremum seeking (ES) algorithm, which optimizes the rise time of the output voltage of a high voltage converter modulator (HVCM) at the Los Alamos Neutron Science Center by iteratively, simultaneously tuning the first eight switching edges of each of the three-phase drive waveforms (24 variables total). We achieve a 50 μs rise time, which is reduction in half, compared to the 100 μs achieved at the Spallation Neutron Source at Oak Ridge National Laboratory. Considering that HVCMs typically operate with an output voltage of 100 kV, with a 60-Hz repetition rate, the 50 μs rise time reduction will result in very significant energy savings. The ES algorithm will prove successful, despite the noisy measurements and cost calculations, confirming the theoretical results that the algorithm is not affected by noise whose frequency components are independent of the perturbing frequencies.**

***Index Terms*— Adaptive control, automatic voltage control, linear particle accelerator, nonlinear circuits, nonlinear control systems, pulse power systems.**

I. Introduction

A. Motivation

Particle accelerators are essential for research in a wide range of fields, including everything from fundamental high-energy physics to the study of material properties and chemical reactions. As the required output particle energy of accelerators has increased to a range of MeV to TeV, modern particle accelerating structures have been able to limit their length to a range of one to tens of kilometers by operating with accelerating electric fields whose voltage gradients are on the MV/m scale. Because such high gradients are not possible in DC systems, in which breakdown and arcing will destroy the fields and damage the accelerating structures, the use of resonant cavities, whose standing electromagnetic fields typically resonate at hundreds of megahertz, is required. To provide the energy needed to excite such accelerating cavities, there is a requirement for high power radio-frequency (RF) sources.

Modern particle accelerators utilize Klystrons, high frequency oscillators/amplifiers, as their RF sources [1]. The RF output of a Klystron must meet very stringent repeatability and stability constraints so that the cavities they power accelerate all particles by very precise amounts. Particles traveling too fast or too slow no longer match the very energy-dependent design of the accelerating structure. The Klystrons must therefore have very stable, very repeatable high voltage sources, such as high voltage converter modulators (HVCM), which convert the energy stored in capacitor banks to large, flat voltage pulses. The growing popularity of HVCMs is due to the significant performance advantages that they offer over conventional modulator technologies for long pulse applications [2], [3]. These include high efficiency, low stored energy, and small size and cost. HVCMs are capable of providing extremely large output voltages (100 kV) in extremely short periods of time (hundreds of μs), with very repeatable and stable, "flat-top" output waveforms ($< 1\%$ error).

While the steady state operation of HVCMs is well understood and there exist analytic results for flat top operation, including droop compensation [2], [4], the dynamics of the voltage rise time are complicated. Even if HVCM output voltage rise could be well described analytically, being a function of up to 24 parameters, its optimization (fast rise time, no overshoot) is a challenging task. For example, at Oak Ridge National Laboratory, the HVCM pulses are gently initialized with one phase activated at a time, resulting in acceptable overshoot levels and a rise time of approximately 100 μs. Therefore, in the experiment that is the subject of this paper, extremum seeking (ES) was utilized for output voltage optimization in the sense of decreasing rise time, while preventing dangerous overshoot.

The ES method, a real-time non-model-based optimization approach, for use in maximizing cost functions based on stable systems, has seen significant theoretical advances during the past decade, including the proof of local convergence [5]–[8], with extension to semi-global convergence [9]. Recent theoretical advances [10], [11] have developed a modified ES algorithm, extending the application from optimization searching of stable systems to perturbation-driven optimum searching as well as real time stabilizing feedback of unstable, unknown systems with unknown control direction.

Earlier forms of ES have been used in diverse applications with unknown/uncertain systems, such as steering vehicles toward a source in GPS-denied environments [12]–[14], active flow control [15]–[17], aeropropulsion [18], cooling

Manuscript received June 18, 2012; revised October 16, 2012; accepted January 6, 2013. Manuscript received in final form January 11, 2013. Date of publication February 1, 2013; date of current version December 17, 2013. This work was supported in part by Los Alamos National Laboratory and UCSD. Recommended by Associate Editor M. Guay.

A. Scheinker is with the Los Alamos National Laboratory, Los Alamos, NM 87545 USA, and also with the Department of Aerospace and Mechanical Engineering, University of California at San Diego, La Jolla, CA 92093 USA (e-mail: ascheink@ucsd.edu).

M. Bland and J. Audia are with the Los Alamos National Laboratory, Los Alamos, NM 87545 USA (e-mail: michael.bland@hotmail.co.uk; jaudia@lanl.gov).

M. Krstić is with the Department of Mechanical and Aerospace Engineering, University of California at San Diego, La Jolla, CA 92093 USA (e-mail: krstic@ucsd.edu).

Color versions of one or more of the figures in this paper are available online at http://ieeexplore.ieee.org.

Digital Object Identifier 10.1109/TCST.2013.2240387

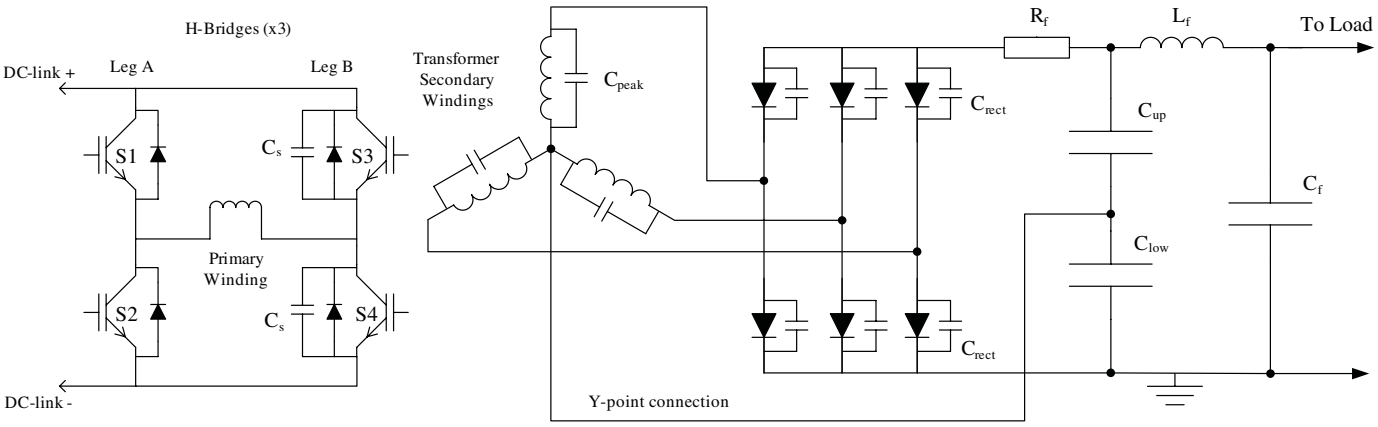

Fig. 1. Simplified schematic diagram of a typical HVCM. The primary windings of the three H-bridges, shown on the left, are connected to the secondary windings in a "Y" shown on the right.

systems [19], [20], photovoltaics [21], human exercise machines [22], wind energy [23], controlling Tokamak plasmas [24], electromechanical valve actuation [25], enhancing mixing in magnetohydrodynamic channel flows [26], beam matching [27], PID gain tuning [28], and laser pulse shaping [29].

B. Results of This Paper

We attempt to optimize the output voltage rise-time of the HVCM at Los Alamos National Laboratory (LANL) to 50 μs by three methods. For each method, we choose (experimentally found) very bad initial parameter settings, so that the system experiences unacceptable overshoot, not settling to acceptable operating conditions until approximately 200 μs into the pulse.

In the first approach, we iteratively tune the first six switching edges of each of the three-phase drive waveforms (18 variables total) of the HVCM by a simple update law based on a noisy cost function, which is calculated from sampled raw data of the HVCM's output voltage. Despite the presence of random noise in the data input to the cost function, because the noise is independent from the perturbing frequencies of the ES algorithm, the output voltage is brought within 2% error of the desired output level in approximately 10 min of run time.

In the second approach, we again iteratively tune the first six switching edges of each of the three-phase drive waveforms of the HVCM, but use an average of five output voltage waveforms, which are created by firing the HVCM five times with fixed input parameters to calculate a smoother cost function. While averaging reduces random noise in the cost function, it slows down the iterative process. With the cleaner cost function, output voltage is brought within approximately 1.5% error of the desired output level, in approximately 30 min of run time.

In the third approach, we increase the number of tuned parameters from the first six to the first eight switching edges of each of the three-phase drive waveforms (24 variables total) of the HVCM, and also increase averaging from five to ten output voltage waveforms, which are created by firing the HVCM ten times with fixed input parameters to calculate an even smoother cost function. Although the averaging used to reduce random noise in the cost function slows down the iterative process, an hour long tune up is more than acceptable because once the input parameters have been optimized, they are set and maintained at the optimal settings. With the cleaner cost function, the output voltage is successfully brought within 1% error of the desired output level, in approximately 60 min of run time.

The ES algorithm is implemented in real-time computer code, running on an embedded hardware platform based on the Texas Instruments TMS320F28335 Digital Signal Controller. Compared to the currently achievable rise time of 100 μs for the HVCMs at the Spallation Neutron Source at Oak Ridge National Laboratory, the improvement achieved is a 2$\times$ reduction. Considering that HVCMs run at 100 kV with 60-Hz repetition rates, the 50-μs rise time reduction will lead to very significant energy savings and higher repetition rate.

C. Organization

In Section II, we give a brief overview of the theory of operation of a high voltage converter modulator. In Section III, we give a brief overview of theory behind the perturbation based extremum seeking method. In Section IV, we present our HVCM ES algorithm. In Section V, we present the results of our experiments.

II. Background on High Voltage Converter Modulator Operation

The first generation of HVCMs was developed at the Los Alamos National Laboratory for the Spallation Neutron Source (SNS) at Oak Ridge National Laboratory. High HVCMs offer significant performance advantages over conventional modulator technologies for long pulse applications [2], [3]. These include high efficiency, low stored energy, and small size and cost.

A simplified schematic diagram of a typical HVCM is shown in Fig. 1. Direct modulation of a switching power supply is used to produce the pulse. A high frequency transformer incorporated into the supply is used to move from voltages suitable for the semiconductors, to those required by the load. Three input H-Bridges (only one is shown in Fig. 1) are connected to a common DC-link capacitor (not shown).

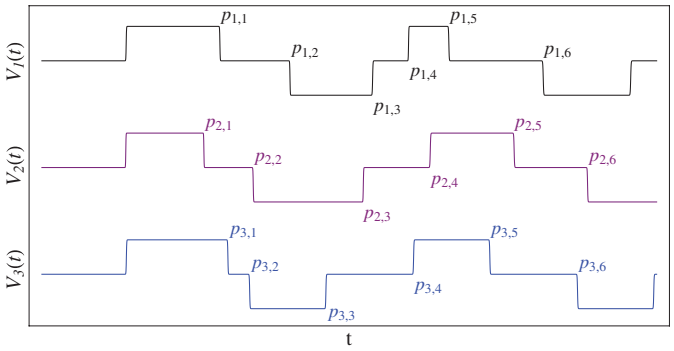

Fig. 2. $p_{i,j}$ is the j^{th} switching edge of the i^{th} drive waveform V_i of each of the three input H-Bridges (as shown in Fig. 1). The extremum seeker tunes only the first six switching edges of each drive waveform, which influence the rise time. The other waveforms are maintained at pre-calculated values.

The output of each H-Bridge is connected to the primary winding of a high voltage transformer. The transformer secondary windings are connected in "Y" and to the output rectifier and filter.

A steady state analysis of the HVCM is presented in [4]. However, the interaction between the high frequency resonant components and the output filter makes it very difficult to analyze the circuit under transient conditions. Therefore, in order to optimize the rise time of the output voltage across the load, the first few switching edges of the three-phase drive waveforms of each of the three input H-Bridges (as shown in Fig. 2) were perturbed according the extremum seeking scheme outlined in this paper.

III. Extremum Seeking Method

Typically, the ES method is utilized for minimization of a cost based on the output of a stable system of unknown dynamics by adding perturbations to the system's input. The basic idea is that given an unknown function $F(x)$ and an estimate x_0 of a locally minimizing input x^*, we add a periodic perturbation to the input, so that the input has the form $x(t) = x_0 + \sin(\omega t)$. We then observe the influence of the oscillations on the value $F(x_0 + \sin(\omega t))$ of the unknown function, with the ES algorithm extracting information regarding the gradient. By estimating the gradient as positive or negative, the ES algorithm pushes $F(x)$ toward the local minimum $F(x^*)$. This basic idea behind the perturbation-based extremum seeking scheme is shown in Fig. 3.

IV. Extremum Seeking Algorithm for HVCM

In order to apply the ES method to the HVCM, we must first define a cost function and input parameters, which we perturb in order to minimize the given cost. Toward this end, we first develop the following mathematical description of the dynamics and measurements of the HVCM's outputs that are of interest to us.

We consider the operation of the HVCM on two time scales, t and s. The time t is the actual time and $n \in \mathbb{N}$ is the iteration number, which in this case we consider to be an independent time scale from the viewpoint of the digital controller, as described in more detail below. Relative to t, the HVCM

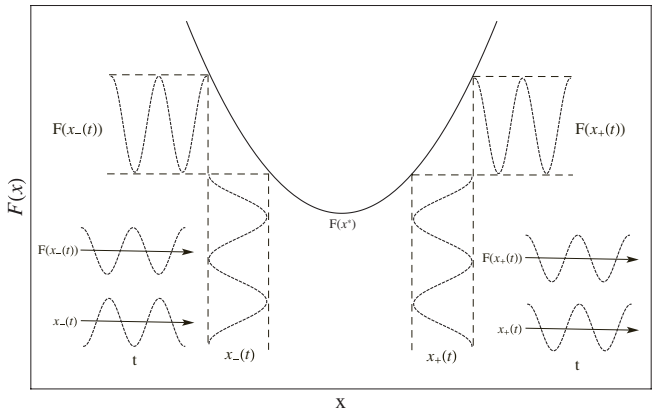

Fig. 3. Near the minimizer x^* of an unknown function $F(x)$, if we periodically oscillate $x_+(t) > x^*$, we see that $x_+(t)$ and $F(x_+(t))$ are in phase and so, the integral of their product is a positive quantity. If instead we periodically oscillate $x_-(t) < x^*$, we see that $x_-(t)$ and $F(x_-(t))$ are out of phase and so, the integral of their product is a negative quantity.

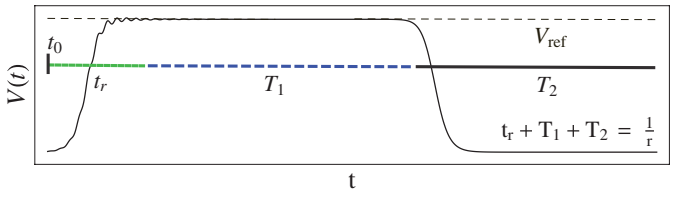

Fig. 4. HVCM is periodically activated with rise time t_r and pulse width T_1 defined such that $|V(t) - V_{\text{ref}}| < (|V_{\text{ref}}|/100)$ for all $t \in [t_r, t_r + T_1]$. The HVCM is then turned off for a length of time T_2 such that the period T of one operation cycle is equal to $t_r + T_1 + T_2 = \frac{1}{r}$, resulting in r pulse per second.

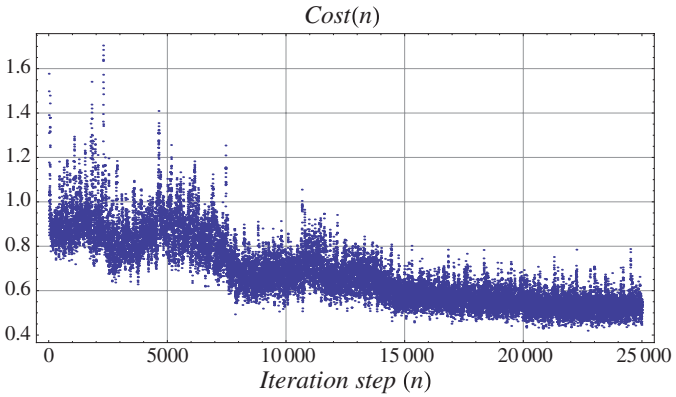

Fig. 5. Noisy cost calculated in the digital signal processor due to noisy data during $n = 25\,000$ iterative steps.

is operated in a periodic fashion with an operator-prescribed repetition rate of r (typically 60 Hz), as outlined in Fig. 4. The operator defines a desired output voltage V_{ref} and pulse length T_1. At any t_0, with output voltage $V(t_0) = 0$, the HVCM is initialized, and the output voltage begins to rise until $t = t_0 + t_r$ at which time 1% error is reached and maintained relative to the desired reference voltage for a time of T_1 so that $|V(t) - V_{\text{ref}}| < (|V_{\text{ref}}|/100)$ for all $t \in [t_0 + t_r, t_0 + t_r + T_1]$. At $t = t_0 + t_r + T_1$ the HVCM is turned off and the output voltage quickly drops to 0, and stays off for a time length of T_2, during which calculations and parameter updates may take place. T_2 is chosen such that $\frac{1}{r} = T = t_r + T_1 + T_2$, resulting in

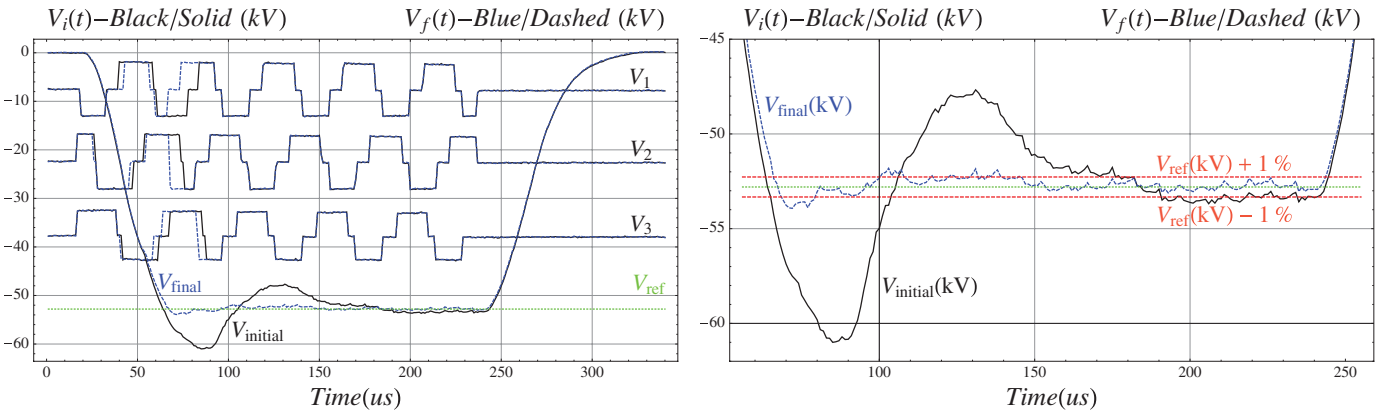

Fig. 6. Under the initial scheme, without averaging and using only six edges per driving waveform, the final output voltage was within 2% error after extremum seeking was completed. V_{initial}, V_{final}, and V_{ref} are shown in units of kV, the driving waveforms V_1, V_2, and V_3 are shifted and dilated for comparison. Black solid lines: initial settings. Blue dashed lines: final settings.

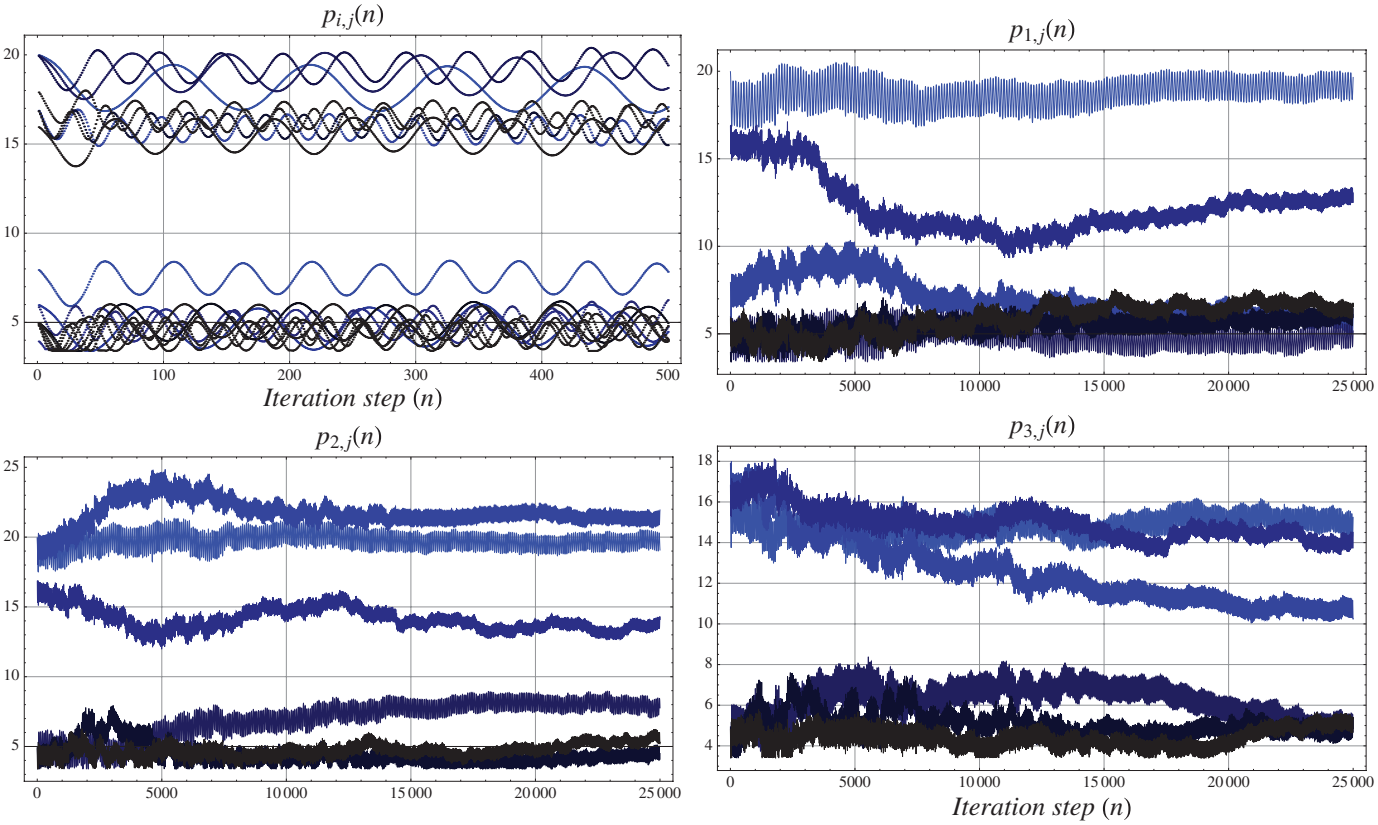

Fig. 7. Motion of the switching edges of the driving waveforms V_1, V_2, and V_3 is shown during the extremum seeking optimization. At the top, we zoom in on the initial $n = 500$ steps to show the smooth oscillation of all 18 parameters, each at their own perturbing frequency. Pulse widths are shown in microseconds.

r pulse per second of pulse-width T_1. The HVCM's operation timing is linked to the accelerator's master timing system, so that the Klystrons fill the resonant accelerating cavities with electromagnetic fields for beam acceleration.

The dynamics of the output voltage V of the HVCM may, therefore, be described by a $\frac{1}{r} = T$-periodic system

$$\frac{\partial V(n,t)}{\partial t} = F\left(V, P(n), t\right) = F\left(V, P(n), t+T\right) \quad (1)$$

where $V(n, t_0) = V(n, t_0 + T) = 0$ and F is some nonlinear function describing the dynamics of the circuit in Fig. 1.

Although it is possible to simulate the performance of the HVCM and to provide an analytic description of the steady-state behavior [2], there is no analytic model describing the dynamics of the HVCM and thereby a relationship between the positions of the switching edges of the three-phase drive waveforms of each of the three input H-Bridges to the transient behavior of the output voltage. In this sense, F is an unknown function of the 18 parameters

$$\begin{bmatrix} p_{1,1}(n) & p_{1,2}(n) & p_{1,3}(n) & p_{1,4}(n) & p_{1,5}(n) & p_{1,6}(n) \\ p_{2,1}(n) & p_{2,2}(n) & p_{2,3}(n) & p_{2,4}(n) & p_{2,5}(n) & p_{2,6}(n) \\ p_{3,1}(n) & p_{3,2}(n) & p_{3,3}(n) & p_{3,4}(n) & p_{3,5}(n) & p_{3,6}(n) \end{bmatrix}$$

which we have grouped as $P(n)$, with each $p_{i,j}(n)$ being the j^{th} switching edge of the i^{th} drive waveform V_i of the three input H-Bridges as shown in Fig. 2. $V(n,t)$ is the measurable HVCM output voltage at time t for parameter settings $p_{i,j}(n)$, where n is independent of t, as discussed in more detail below.

For any $t \in [t_0, t_0+t_r+T_1]$, the output voltage has dynamics as described by (1), and values

$$V(n,t) = \int_{t_0}^{t_0+t} F\left(V(n,\tau), P(n), \tau\right) d\tau$$
$$V(n,t) = 0, \ \ t \in [t_0 + t_r + T_1, T].$$

For $t \in [t_0 + t_r + T_1, t_0 + t_r + T_1 + T_2]$, the embedded hardware has T_2 seconds to perform calculations and update the parameter values $p_{i,j}(n)$.

Based on the results of [10], in order to minimize a cost function, as suggested by the Lie bracket, averaging results (discussed in more detail below) the iterative tuning law for the parameters $p_{i,j}(n)$ is chosen as

$$\begin{aligned} p_{i,j}(n+1) = \ & p_{i,j}(n) + \alpha\sqrt{\omega_{i,j}}\cos\left(\omega_{i,j}ndn\right)dn \\ & -k\sqrt{\omega_{i,j}}\sin\left(\omega_{i,j}ndn\right)C(n)dn \end{aligned} \tag{2}$$

where we have defined the cost function

$$C(n) = \int_{t_1}^{t_2} \left(V(n,\tau) - V_{\text{ref}}\right)^2 d\tau \tag{3}$$

where t_1 is the desired rise time, and t_2 is chosen such that $t_1 < t_2 \leq T_1$ and is a long enough time so that the system has reached steady state.

Note 1: The update law (2) also has rules, which do not let the system do something nonphysical, such as placing two switching edges on top of each other. A few of the many cases of such a rule are given as: If $p_{i,j}(n+1) = p_{i,j+1}(n+1)$, then $p_{i,j}(n+1) = p_{i,j}(n)$. If $p_{i,1}(n+1) < 0$, then $p_{i,1}(n+1) = p_{i,1}(n)$.

The update law (2) is chosen with $dn \ll 1$ sufficiently small relative to the perturbation periods $T_{i,j} = \frac{2\pi}{\omega_{i,j}}$ so that based on the finite difference approximation of a derivative, the system's n-dynamics approximately satisfy

$$\frac{\partial p_{i,j}}{\partial n} = \alpha\sqrt{\omega_{i,j}}\cos\left(\omega_{i,j}n\right) - k\sqrt{\omega_{i,j}}\sin\left(\omega_{i,j}n\right)C \tag{4}$$

$$\frac{\partial C}{\partial n} = \sum_{i,j=1}^{m}\frac{\partial C}{\partial p_{i,j}}\sqrt{\omega_{i,j}}\left(\alpha\cos(\omega_{i,j}n) - k\sin(\omega_{i,j}n)C\right). \tag{5}$$

We briefly recall the Lie bracket averaging technique as developed by Gurvits and Li [30]–[32]. Given a system of the form

$$\dot{x} = \sum_{k=1}^{m_1} b_k(x)\bar{u}_k(t) + \sum_{i=1}^{m_2} b_i(x)\frac{1}{\sqrt{\epsilon}}\hat{u}_i(t,\theta) \tag{6}$$

we can relate to (6) the Lie bracket averaged system

$$\dot{\bar{x}} = \sum_k b_k(\bar{x})\bar{u}_k(t) + \frac{1}{T}\sum_{i<j}[b_i, b_j](\bar{x})v_{i,j}(t) \quad \bar{x}(t_0) = x(t_0) \tag{7}$$

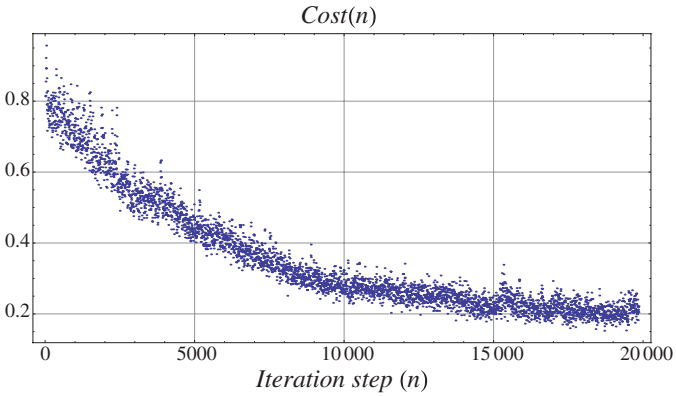

Fig. 8. Less noisy cost was detected in the computer in $n = 20\,000$ steps when each iterative extremum seeking step calculated the cost based on the average of five HVCM shots with fixed settings.

where

$$v_{i,j}(t) = \int_0^T \int_0^\theta \hat{u}_i(t,\tau)\hat{u}_j(t,\theta)d\tau d\theta$$
$$\left[b_i, b_j\right] = \frac{\partial b_j}{\partial \bar{x}}b_i - \frac{\partial b_i}{\partial \bar{x}}b_j$$

such that the two systems satisfy the property that for any $\hat{T} > 0$ and $\delta > 0$, there exists $\epsilon^\star$ such that for all $\epsilon \in (0, \epsilon^\star)$ $\forall t \in [t_0, t_0 + \hat{T}]$ for all $x(t) \in D$

$$|x(t) - \bar{x}(t)| < \delta. \tag{8}$$

Therefore, by considering each $\frac{1}{\omega_{i,j}}$ as a small parameter $\epsilon_{i,j}$, we can associate with system (4), (5) the averaged system

$$\frac{\partial \bar{C}}{\partial n} = -\frac{k\alpha}{2}\sum_{i,j=1}^{m}\left(\frac{\partial \bar{C}}{\partial p_{i,j}}\right)^2, \quad \bar{C}(n_0) = C(n_0) \tag{9}$$

$$\frac{\partial \bar{p}_{i,j}}{\partial n} = -\frac{k\alpha}{2}\frac{\partial \bar{C}}{\partial \bar{p}_{i,j}}, \quad \bar{p}(n_0) = p(n_0) \tag{10}$$

which exponentially converges to a local minimum of the cost function $\bar{C}$. The relationship between C and $\bar{C}$ is such that for a given n-time length $\hat{N}$ and a desired accuracy $\delta > 0$, there exists $\omega^\star$ such that for all $\omega > \omega^\star$

$$\left|C(n) - \bar{C}(n)\right| < \delta, \quad \forall n \in \left[n_0, n_0 + \hat{N}\right]. \tag{11}$$

Remark 1: On the choices of ω, k, and α.

The term $\alpha\sqrt{\omega_{i,j}}\cos\left(\omega_{i,j}n\right)$ in (4) can be thought of as the perturbing dither term in classical extremum seeking methods. Unlike the $-k\sqrt{\omega_{i,j}}\sin\left(\omega_{i,j}n\right)C(n)$ term, which decreases with decreased cost, the α term is always present, with an amplitude of (after integration) $\frac{\alpha}{\omega_{i,j}}$. Therefore, either a very small value of α or a very large value of the $\omega_{i,j}$ is required in order for the tuned parameters $p_{i,j}$ to settle near optimal set-points as the cost function is minimized. Simply choosing a very small value of α introduces difficulties because the overall system, on average, converges at a rate proportional to the product $k\alpha$. Therefore, in practice, a reasonable α is first chosen (by trial and error) and then a much larger value of k is also chosen, so that the product $k\alpha$ gives reasonably fast convergence, with the large k term vanishing as the cost function is decreased. The value of the $\omega_{i,j}$ is increased until

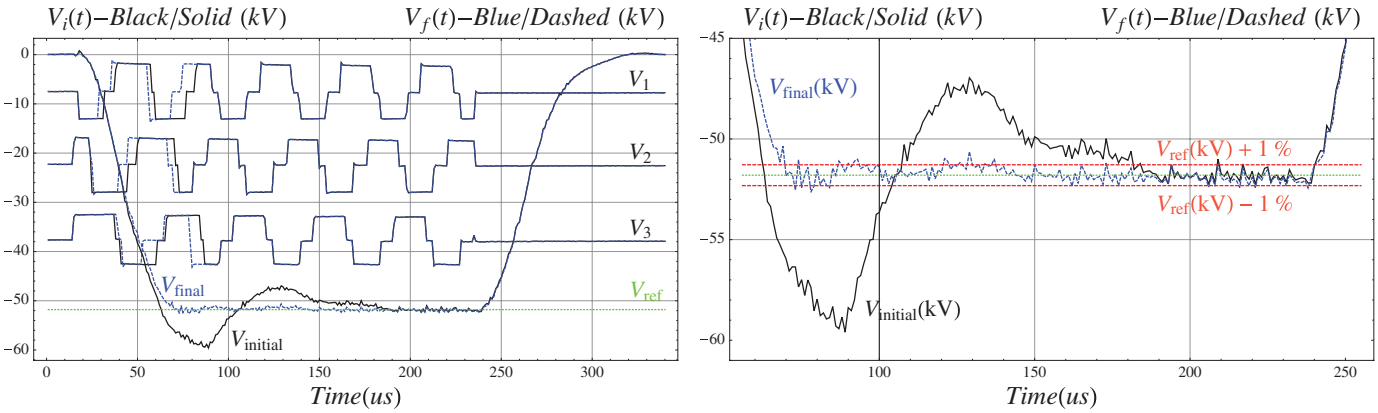

Fig. 9. Using the averaging scheme and six edges per driving waveform, the final output voltage was closer, but still not completely within 1% error after extremum seeking was completed. V_{initial}, V_{final}, and V_{ref} are shown in units of kV, the driving waveforms V_1, V_2, and V_3 are shifted and dilated for comparison. Black solid lines: initial settings. Blue dashed lines: final settings.

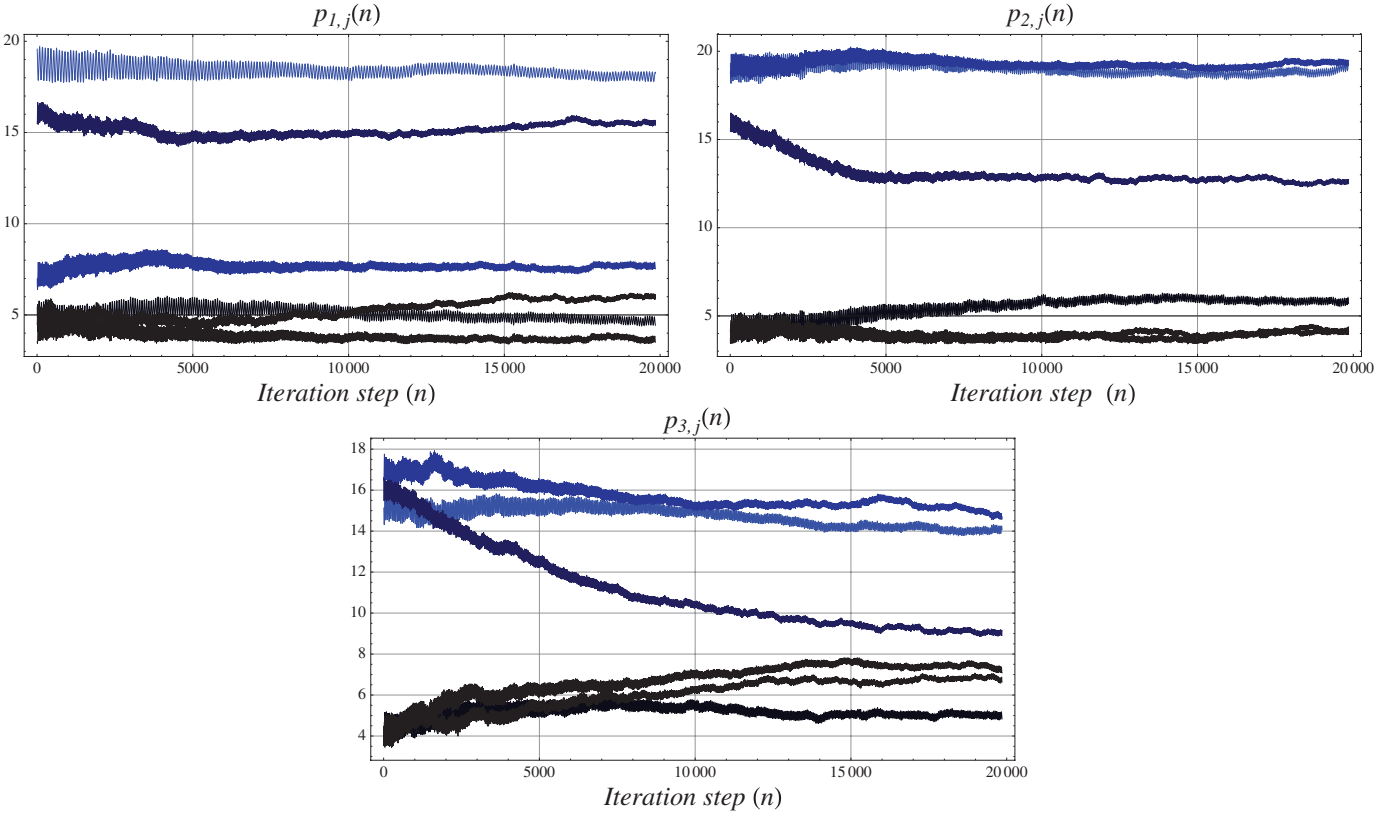

Fig. 10. Evolution of the switching edges of the driving waveforms V_1, V_2, and V_3 during the extremum seeking optimization. Pulse widths are shown in microseconds.

stability and a desired level of convergence (relative to the size of α) is achieved.

Theoretically, the choices of $\omega_{i,j}$ must be distinct to satisfy the requirements of the Lie bracket averaging. In practice, the choices of $\omega_{i,j}$ should further satisfy the property that for all distinct $\omega_{i,j}$, $\omega_{i_1,j_1} \neq \omega_{i_2,j_2} \pm \omega_{i_3,j_3}$, to prevent mixed signals in the nonlinear system from creating harmonics, which cause cross talk between different components. In the experiment, it was found that using perturbing frequencies of the form $\omega_{i_1,j_1} = 2\omega_{i_2,j_2}$ cause the system to periodically experience large disturbances. One simple method for choosing the perturbing frequencies was picking $\omega_{i,j} = \omega_0\sqrt{\Omega_{i,j}}$, where ω_0 was a fixed large scaling factor, and the $\Omega_{i,j}$ were numbers with irrational square roots. Although the numbers were truncated, removing all decimal components, the scheme successfully removed harmonic dependence among signals.

In order for the analysis and application presented here to be useful, to ensure that the averaged cost $\bar{C}(n)$ reaching a local minimum implies that the actual cost $C(n)$ also reaches a small neighborhood of a local minimum, the relationship in (11) must hold for a sufficiently small δ and sufficiently large $\hat{N}$. The frequencies $\omega_{i,j}$ must be large relative to the values of k and α and independent of the frequency components of any persistent noise present in the cost function measurements.

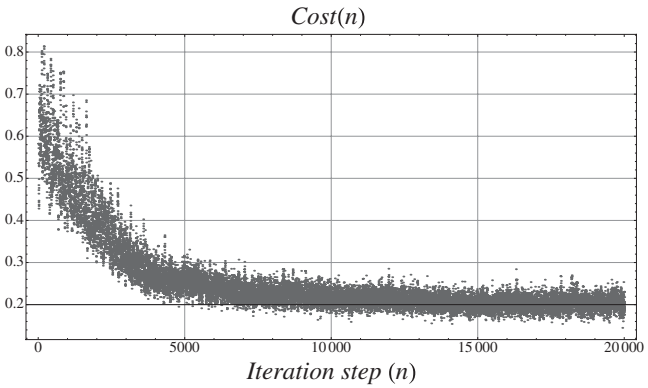

Fig. 11. Less noisy cost was detected in the computer in $n = 20\ 000$ steps when each iterative extremum seeking step calculated the cost based on the average of ten HVCM shots with fixed settings. More term averaging combined with more perturbed edges allowed the cost to reach a lower value than the previous two schemes, resulting in the best output voltage waveform.

Implementing the described controller with large values of $\omega_{i,j}$ is not problematic. The algorithm is implemented iteratively and the high frequency $\left(f_{i,j} = \frac{\omega_{i,j}}{2\pi}\right)$ perturbations are only of high frequency relative to the parameter n, which is independent of actual time. The value n is only a digital parameter, the system itself does not oscillate, but is implemented at fixed settings of $p_{i,j}(n)$ for a given time period of T with only the digital update law (2) experiencing fast oscillations. Once $C(n)$ has reached a desired level at some iteration n_2, the extremum seeker is turned off, with parameter settings fixed at the constant values $p_{i,j}(n > n_2) \equiv p_{i,j}(n_2)$.

V. Experimental Results

Experimental results have confirmed the ability of the extremum seeking algorithm to optimize the output voltage rise-time of the HVCM at LANL to 50 μs, providing a reduction in half compared to the 100 μs achieved at SNS. Furthermore, the results confirm the ability of the ES scheme to handle noisy measurements, as long as the noise does not have frequency components, which correlate to the perturbing frequencies.

Throughout the experiments, the desired output voltage was set at $V_{\text{ref}} = -10$ kV, a voltage low enough to allow a 60-Hz repetition rate with the available load. After optimization, with parameters fixed at their optimal settings, the voltage was turned up to approximately -50 kV, and the HVCM was again triggered to generate a pulse and confirm the desired output voltage performance.

Following three separate experiments, which are discussed in detail below, the HVCM was fired at -90 kV, a quantity limited by both the available power sources and current load setup, confirming $< 1\%$ error.

A. Six Edges Per Phase, Noisy Cost Function

In the first application of the ES algorithm, we iteratively tune the first six switching edges of each of the three-phase drive waveforms (18 variables total) of the HVCM with a rep rate of 60 Hz, which was limited by the available load. Optimization took place by the simple update law given by (2), with the cost calculated as given in (3), where $t_1 = 40$ μs, $t_2 = 100$ μs is sufficiently large to capture voltage transients, $k = 500$, $\alpha = 0.1$, and the voltage output $V(t, n)$ depends on the parameter settings $p_{i,j}(n)$ at step n. The perturbing angular frequencies $\omega_{i,j}$ of the parameters $p_{i,j}$ are chosen as

$$\begin{bmatrix} 115537 & 142643 & 164579 & 181076 & 199467 & 213282 \\ 229667 & 243898 & 256839 & 296917 & 319432 & 339395 \\ 378375 & 399167 & 413745 & 433573 & 455621 & 488106 \end{bmatrix}$$

and $\delta = 5 \times 10^{-7}$, so that $\frac{\max_{i,j}\{\omega_{i,j}\}}{2\pi}\delta < \frac{1}{30}$, guaranteeing that on the n-time scale, the sines and cosines are smooth, with at least 30 points per 2π phase advance for the highest frequency. The evolution of the cost function $C(n)$ over $n = 25\ 000$ iterative steps, which is 25 000 $T \approx 5$ min of real time optimization is shown in Fig. 5. While keeping the parameters $p_{i,j}$ fixed at the values optimized for -10 kV, the voltage is then turned up to -52.8 kV, and a comparison of the initial and final output voltage waveforms is shown in Fig. 6. Voltage output error was reduced to less than 2%. Fig. 7 shows the evolution of the perturbed pulse widths (in microseconds) of the driving waveform V_1, V_2, and V_3 during the extremum seeking optimization process.

B. Six Edges Per Phase, Averaged Cost Function

With the cost as noisy as it is shown in Fig. 5, a slightly different extremum seeking scheme was attempted, in which parameters were set and the HVCM was fired 5 times allowing the five output voltage waveforms to be averaged in order to calculate the cost, smoothing out random perturbations. In order to converge more closely to a minimum, at the expense of slower convergence, the value of α was decreased to 0.01. Again, initially we set $V_{\text{ref}} = -10$ kV so that we can iteratively tune the first six switching edges of each of the three-phase drive waveforms (18 variables total) of the HVCM with a rep rate of 60 Hz, which was limited by the available load. Optimization took place by the same update law (2), with the cost replaced by an averaged value $\bar{C}(n)$, which is calculated by averaging five cost measurements $C(n_1), \ldots, C(n_5)$, each calculated as

$$C(n_i) = \int_{t_1}^{t_2} (V(n_i, \tau) - V_{\text{ref}})^2 \, d\tau \tag{12}$$

where the parameters $p_{i,j}(n_l)$ were kept constant during the five averaging shots $n_1, \ldots, n_5$, where again $t_1 = 50$ μs, $t_2 = 100$ μs is sufficiently large to capture voltage transients, $k = 400$, $\alpha = 0.01$, and the voltage output $V(t, n)$ depends on the parameter settings $p_{i,j}(n)$ at step n. We again chose $\delta = 5 \times 10^{-7}$. The evolution of the cost function $C(n)$ over $n = 20\ 000$ averaged iterative steps (100 000 actual steps), which is 100 000 $T \approx 30$ min of real time optimization, as shown in Fig. 8. The voltage is then turned up to -51.8 kV, and a comparison of the initial and final output voltage waveforms is shown in Fig. 9. The output voltage error, with the smoother cost the output voltage waveform was improved, but was still outside of the desired $< 1\%$ error range. Fig. 10 shows the evolution of the perturbed pulse widths (in microseconds) of the driving waveform V_1, V_2, and V_3 during the extremum seeking optimization process.

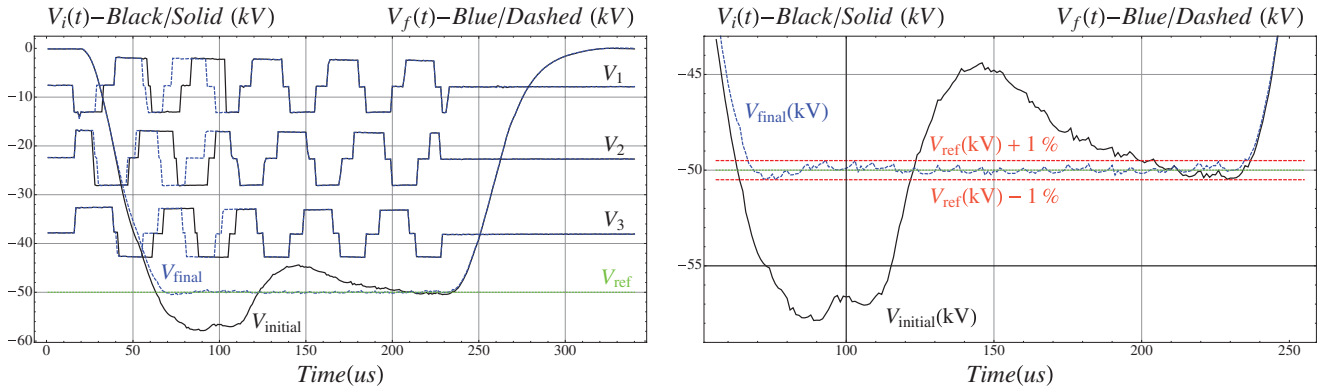

Fig. 12. Using the averaging scheme and eight edges per driving waveform, the final output voltage was within 1% error after extremum seeking was completed. V_{initial}, V_{final}, and V_{ref} are shown in units of kV, the driving waveforms V_1, V_2, and V_3 are shifted and dilated for comparison. Black solid lines: initial settings. Blue dashed lines: final settings.

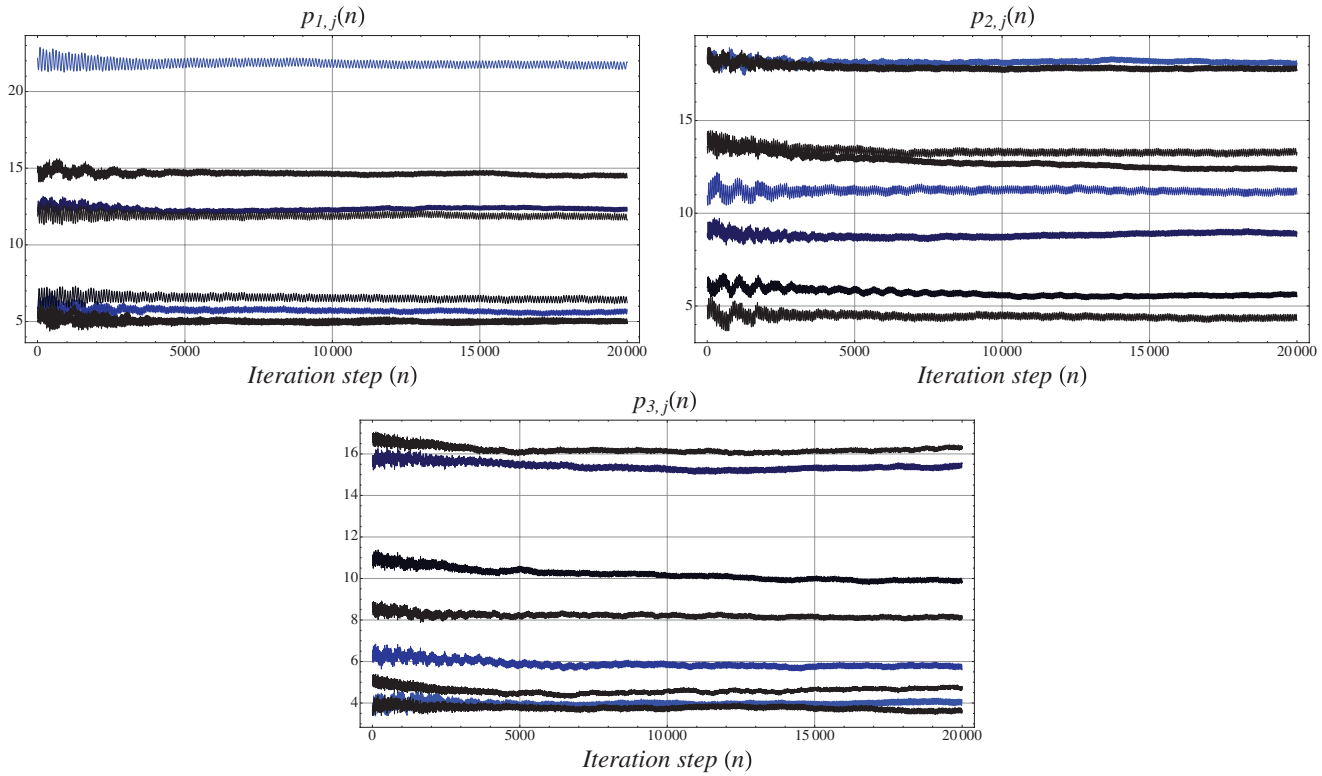

Fig. 13. Evolution of the switching edges of the driving waveforms V_1, V_2, and V_3 during the extremum seeking optimization. Pulse widths are shown in microseconds.

C. Eight Edges Per Phase, Averaged Cost Function

Finally, an extremum seeking scheme was attempted in which parameters were set and the HVCM was fired 10 times, allowing the ten output voltage waveforms to be averaged. A cost calculation based on more averaging helped in smoothing out random perturbations even further. Also, the number of switching edges per drive waveform was also increased to eight, giving the ES controller more influence over some of the bumps showing up later in the output voltage waveform. Again, initially we set $V_{\text{ref}} = -10$ kV so that we can iteratively tune the first eight switching edges of each of the three-phase drive waveforms (24 variables total) of the HVCM with a rep rate of 60 Hz, which was limited by the available load. Optimization again took place by the update law (2), with the cost replaced by an averaged value $\bar{C}(n)$, which is calculated by averaging ten cost measurements $C(n_1), \ldots, C(n_{10})$, each calculated as in (12), where the parameters $p_{i,j}(n_l)$ were kept constant during the ten averaging shots $n_1, \ldots, n_{10}$, where again $t_1 = 50$ μs, $t_2 = 100$ μs is sufficiently large to capture voltage transients, $k = 400$, $\alpha = 0.01$, and the voltage output $V(t, n)$ depends on the parameter settings $p_{i,j}(n)$ at step n. The perturbing angular frequencies $\omega_{i,j}$ of the six additional parameters $p_{i,j}$ were chosen as

$$\begin{bmatrix} 532841 & 576844 \\ 629285 & 664875 \\ 712039 & 754672 \end{bmatrix}$$

and $\delta = 5 \times 10^{-7}$, so that $\max_{i,j}\{\omega_{i,j}\}/2\pi\delta < 1/16$, guaranteeing that on the n-time scale, the sines and cosines are smooth, with at least 16 points per 2π phase advance for the highest frequency. The evolution of the cost function $C(n)$ over $n = 20\ 000$ averaged iterative steps (200 000 actual steps), which is 200 000 $T \approx 1$ hour of real time optimization, is shown in Fig. 11. The voltage is then turned up to -50 kV, and a comparison of the initial and final output voltage waveforms is shown in Fig. 12. The output voltage error, with the smoother cost and additional parameters, has dropped within the desired $< 1\%$ range. Fig. 13 shows the evolution of the perturbed pulse widths (in microseconds) of the driving waveform V_1, V_2, and V_3 during the extremum seeking optimization process.

VI. Conclusion

An extremum seeking algorithm was implemented to simultaneously tune 24 parameters of an unknown, nonlinear dynamic system, successfully decreasing the HVCM output voltage rise time by a factor of 2 to within a 1% error. Furthermore, as shown in the results of Section V-A, the ES algorithm is successful despite a possibly noisy cost function, as long as the noise does not have frequency components that match up with any of the ES algorithm's perturbing frequencies.

References

[1] R. Varian and S. Varian, "A high frequency oscillator and amplifier," *J. Appl. Phys.*, vol. 10, no. 5, pp. 321–327, 1939.

[2] M. J. Bland, J. C. Clare, P. Zanchetta, P. W. Wheeler, and J. S. Pryzbyla, "A high frequency resonant power converter for high power RF applications," in *Proc. 11th Eur. Conf. Power Electron. Appl.*, 2005, pp. 1–10.

[3] W. A. Reass, D. M. Baca, M. J. Bland, R. F. Gribble, H. J. Kwon, Y. S. Cho, D. I. Kim, J. Mccarthy, and K. B. Clark, "Operations of polyphase resonant converter-modulators at the Korean Atomic Energy Research Institute," *IEEE Trans. Dielectron. Electr. Insul.*, vol. 18, no. 4, pp. 1104–1110, Aug. 2011.

[4] M. J. Bland, A. Scheinker, J. Clare, J. Chao, A. Watson, and W. Reass, "Droop compensation with soft switching for high voltage converter modulator (HVCM)," presented at the IEEE Int. Power Modulation High Voltage Conf., San Diego, CA, USA, Jun. 2012.

[5] M. Krstić and H. Wang, "Stability of extremum seeking feedback for general dynamic systems." *Automatica*, vol. 36, no. 4, pp. 595–601, Apr. 2000.

[6] J.-Y. Choi, M. Krstić, K. B. Ariyur, and J. S. Lee, "Extremum seeking control for discrete-time systems," *IEEE Trans. Autom. Control*, vol. 47, no. 2, pp. 318–323, Feb. 2002.

[7] M. A. Rotea, "Analysis of multivariable extremum seeking algorithms," in *Proc. Amer. Control Conf.*, vol 1. Sep. 2000, pp. 433–437.

[8] H.-H. Wang and M. Krstić, "Extremum seeking for limit cycle minimization," *IEEE Trans. Autom. Control*, vol. 45, no. 12, pp. 2432–2437, Dec. 2000.

[9] Y. Tan, D. Nešić, and I. Mareels, "On non-local stability properties of extremum seeking control," *Automatica*, vol. 42, no. 6, pp. 889–903, Jun. 2006.

[10] A. Scheinker and M. Krstić, "A universal extremum seeking-based stabilizer for unknown LTV systems with unknown control directions," in *Proc. Amer. Control Conf.*, Montreal, QC, Canada, Jun. 2012, pp. 1129–1136.

[11] A. Scheinker and M. Krstić, "Maximum-seeking for CLFs: Universal semiglobally stabilizing feedback under unknown control directions," *IEEE Trans. Autom. Control*, to be published.

[12] J. Cochran, E. Kanso, S. D. Kelly, H. Xiong, and M. Krstić, "Source seeking for two nonholonomic models of fish locomotion," *IEEE Trans. Robot.*, vol. 25, no. 5, pp. 1166–1176, Oct. 2009.

[13] J. Cochran and M. Krstić, "Nonholonomic source seeking with tuning of angular velocity," *Trans. Autom. Control*, vol. 54, no. 4, pp. 717–731, 2009.

[14] C. Zhang, D. Arnold, N. Ghods, A. Siranosian, and M. Krstić, "Source seeking with nonholonomic unicycle without position measurement and with tuning of forward velocity," *Syst. Control Lett.*, vol. 56, no. 3, pp. 245–252, Mar. 2007.

[15] K. Kim, C. Kasnakoglu, A. Serrani, and M. Samimy, "Extremum-seeking control of subsonic cavity flow," *Amer. Inst. Aeron. Astron. J.*, vol. 47, no. 1, pp. 195–205, 2009.

[16] R. King, R. Becker, G. Feuerbach, L. Henning, R. Petz, W. Nitsche, O. Lemke, and W. Neise, "Adaptive flow control using slope seeking," in *Proc. 14th IEEE Mediterranean Conf. Control Autom.*, Jun. 2006, pp. 1–6.

[17] L. Henning, R. Becker, G. Feuerbach, R. Muminovic, A. Brunn, W. Nitsche, and R. King, "Extensions of adaptive slope-seeking for active flow control," *J. Syst. Control Eng.*, vol. 222, no. 5, pp. 309–322, Aug. 2009.

[18] O. Wiederhold, L. Neuhaus, R. King, W. Niese, L. Enghardt, B. R. Noack, and M. Swoboda, "Extensions of extremum-seeking control to improve the aerodynamic performance of axial turbomachines," in *Proc. 39th AIAA Fluid Dynamics Conf.*, San Antonio, TX, USA, no. AIAA 2009-4175, 2009.

[19] P. Li, Y. Li, and J. E. Seem, "Extremum seeking control for efficient and reliable operation of air-side economizers," in *Proc. Amer. Control Conf.*, Jun. 2009, pp. 20–25.

[20] Y. Li, M.A. Rotea, G. Chiu, L. Mongeau, and I. Paek, "Extremum seeking control of tunable thermoacoustic cooler," *IEEE Trans. Control Syst. Technol.*, vol. 13, no. 4, pp. 527–536, Jul. 2005.

[21] P. Lei, Y. Li, Q. Chen, and J. E. Seem, "Sequential ESC-based global MPPT control for photovoltaic array with variable shading," *IEEE Trans. Sustain. Energy*, vol. 2, no. 3, pp. 348–358, Jul. 2011.

[22] X. T. Zhang, D. M. Dawson, W. E. Dixon, and B. Xian, "Extremum-seeking nonlinear controllers for a human exercise machine," *IEEE/ASME Trans. Mech.*, vol. 11, no. 2, pp. 233–240, Apr. 2006.

[23] J. Creaby, Y. Li, and J. E. Seem, "Maximizing wind turbine energy capture using multivariable extremum seeking control," *Wind Eng.*, vol. 33, no. 4, pp. 361–387, Jun. 2009.

[24] D. Carnevale, A. Astolfi, C. Centioli, S. Podda, V. Vitale, and L. Zaccarian, "A new extremum seeking technique and its application to maximize RF heating on FTU," *Fusing Eng. Design*, vol. 84, nos. 2–6, pp. 554–558, Jun. 2009.

[25] K. Peterson and A. Stefanopoulou, "Extremum seeking control for soft landing of an electromechanical valve actuator," *Automatica*, vol. 40, no. 6, pp. 1063–1069, 2004.

[26] E. Schuster, L. Luo, and M. Krstić, "MHD channel flow control in 2D: Mixing enhancement by boundary feedback," *Automatica*, vol. 44, no. 10, pp. 2498–2507, Oct. 2008.

[27] E. Schuster, C. Xu, N. Torres, E. Morinaga, C. Allen, and M. Krstić, "Beam matching adaptive control via extremum seeking," *Nuclear Inst. Methods Phys. Res. A*, vol. 581, no. 3, pp. 799–815, Nov. 2007.

[28] N. Killingsworth and M. Krstić, "PID tuning using extremum seeking," *IEEE Control Syst. Mag.*, vol. 26, no. 1, pp. 70–79, Feb. 2006.

[29] B. Ren, P. Frihauf, R. Rafac, and M. Krstić, "Laser pulse shaping via extremum seeking," *Control Eng. Pract.* vol. 20, no. 7, pp. 674–683, 2012.

[30] L. Gurvits, "Averaging approach to nonholonomic motion planning," in *Proc. IEEE. Conf. Robot. Autom.*, vol. 3. May 1992, pp. 2541–2546.

[31] L. Gurvits and Z. Li, "Smooth time-periodic solutions for non-holonomic motion planning," Inst. Int. Education, New York Univ., New York, USA, Tech. Rep. TR-598, 1992.

[32] L. Gurvits and Z. Li, "Smooth time-periodic solutions for non-holonomic motion planning," *Nonholonomic Motion Planning*, Z. Li and J. F. Canny, Eds. Norwell, MA, USA: Kluwer, 1992.

Alexander Scheinker (S'10) received the B.A. degrees in mathematics and physics from Washington University, St. Louis, MO, USA, in 2006, and the M.A. degree in mathematics from the University of California, San Diego, CA, USA, in 2008, where he received the Ph.D. degree in dynamic systems and control from the Mechanical and Aerospace Engineering Department, in 2012.

He has been a Staff Member with the Low Level RF Control Group, Los Alamos National Laboratory, Los Alamos, NM, USA, since 2011. His current research interests include stability of uncertain nonlinear systems, nonlinear dynamics, and various topics in particle accelerator physics.

Mr. Scheinker was a Finalist for the Student Best Paper Award at the American Control Conference in 2012.

Michael Bland received the B.Eng. (Hons.) degree in electrical engineering and the Ph.D. degree with research on matrix converters and resonant topologies from The University of Nottingham, Nottingham, U.K., in 1999 and 2003, respectively.

He was a Research Fellow with the Power Electronics, Machines and Control Group, The University of Nottingham, in 1999, where he was involved in research on power supplies for high-power RF applications. From 2009 to 2012, he was a Visiting Scholar with the Los Alamos National Laboratory, Los Alamos, NM, where he was engaged in implementing a novel high-voltage converter modulator design for long-pulse applications with droop compensation. His current research interests include power-circuit design, power-circuit topologies, and resonant-conversion techniques.

Miroslav Krstić (S'92–M'95–SM'99–F'02) received the Ph.D. degree from University of California, Santa Barbara, CA, USA, in 1994.

He was an Assistant Professor with the University of Maryland, College Park, USA, until 1997. He was the Alspach Edowed Chair and is currently the Founding Director of the Cymer Center for Control Systems and Dynamics, University of California, San Diego, CA, USA. He was a Springer Distinguished Visiting Professor of mechanical engineering with the University of California, Berkeley, CA, USA. He has co-authored nine books, including *Stabilization of Nonlinear Uncertain Systems* (Springer, 1998), *Flow Control by Feedback* (Springer, 2002), *Nonlinear and Adaptive Control Design* (Wiley, 1995), *Real-time Optimization by Extremum Seeking Control* (Wiley, 2003), *Control of Turbulent and Magnetohydrodynamic Channel Flows* (Birkhauser, 2007), *Boundary Control of PDEs* (SIAM, 2008), *Delay Compensation for Nonlinear, Adaptive, and PDE Systems* (Birkhauser, 2009), *Adaptive Control of Parabolic PDEs* (Princeton University Press, 2009), and *Stochastic Averaging and Stochastic Extremum Seeking* (Springer, 2012).

Dr. Krstic was a recipient of the Axelby and Schuck Paper Prizes, the NSF Career Award, the ONR Young Investigator Award, and the PECASE Award. He is a fellow of IFAC.

Jeff Audia is currently an Embedded Systems Hardware and Software Developer involved in research on microelectronics, computer programming, circuit design, and fabrication. He is currently with the AOT-RFE Group, Los Alamos Neutron Science Center, Los Alamos National Laboratory, Los Alamos, NM, USA, where he is involved in research on instrumentation and control electronics for power conversion and pulsed-power applications.